Carbohydrate Polymers 89 (2012) 842–848

Contents lists available at SciVerse ScienceDirect

Carbohydrate Polymers

journal homepage: www.elsevier.com/locate/carbpol

Chitosan-functionalized poly(methyl methacrylate) particles by spinning disk processing for lipase immobilization

Somkieath Jenjob[a,b], Panya Sunintaboon[a,b,*], Pranee Inprakhon[c], Natthinee Anantachoke[b,d], Vichai Reutrakul[b]

[a] Department of Chemistry, Faculty of Science, Mahidol University, 999 Phuttamonthon 4 Road, Salaya, Nakhon Pathom 73170, Thailand
[b] Center of Excellence for Innovation in Chemistry (PERCH-CIC), Department of Chemistry, Faculty of Science, Mahidol University, Rama 6 Road, Bangkok 10400, Thailand
[c] Department of Biotechnology, Faculty of Science, Mahidol University, Rama 6 Road, Bangkok 10400, Thailand
[d] Center of Excellence for Innovation in Chemistry (PERCH-CIC), Department of Pharmacognosy, Faculty of Pharmacy, Mahidol University, Rama 6 Road, Bangkok 10400, Thailand

ARTICLE INFO

Article history:
Received 10 January 2012
Received in revised form 7 April 2012
Accepted 7 April 2012
Available online 26 April 2012

Keywords:
Poly(methyl methacrylate)
Chitosan
Core–shell particle
Lipase immobilization
Spinning disk processing

ABSTRACT

Chitosan-functionalized poly(methyl methacrylate) (PMMA-CH) particles were prepared by complexation between the negatively charged PMMA particles and the positively charged chitosan *via* a spinning disk processing. Processing parameters; feed rate and spinning speed, were optimized, which were traced by size distribution profiles of the formed PMMA-CH particles. Their sizes and net surface charges were found to be affected by MWs of chitosan (45, 100, and 230 kDa) used. Microscopic evidences were used to confirm their core–shell morphology. Chemical characteristics and thermal stability of such particles were determined by FTIR and TGA, respectively. Then, their ability to immobilize lipase (EC 3.1.1.3) was conducted and followed through zeta potential measurement. The percentage of lipase adsorption capacity increased with increasing lipase content, but the value decreased when the size of PMMA-CH particles increased. Also, the activity of lipase attached on PMMA-CH particles' surface was preserved and increased with lipase loading.

© 2012 Elsevier Ltd. All rights reserved.

1. Introduction

Chitosan is a naturally occurring polymer obtained by partial deacetylation of chitin, a main structural component of cuticles of crustaceans. It is insoluble in water, but becomes soluble and positively charged in acidic media (Marie, Landfester, & Antonietti, 2002). Due to its biodegradability, biocompatibility, and renewability, chitosan has been used in a wide range of applications (Jia et al., 2011). In addition, this polymer has been used successfully to colloidally stabilize polymer nanoparticles, such as poly(methyl methacrylate), or polystyrene nanoparticles (Caruso, Lichtenfeld, Giersig, & Mohwald, 1998; Li, Zhu, Sunintaboon, & Harris, 2002). Nowadays, chitosan-decorated materials attract much attention because they could be used in diverse aspects such as controlled release systems of drugs, antibiotics, or biological active agents (Torrado, Prada, De la Torre, & Torrado, 2004), particularly when chitosan was cross-linked with genipin (Muzzarelli, 2009). Moreover, chitosan has also been used as a matrix for lipase immobilization since it has numerous amine groups, which can interact with enzyme (Chiou & Wu, 2004; Muzzarelli, Francescangeli, Tosi, & Muzzarelli, 2004). This methodology is very simple and improves enzyme stability significantly. Chitosan is also recognized by its excellent properties for lipase support such as biocompatibility, biodegradability, nontoxicity, physiological inertness, and great affinity for proteins (Krajewska, 2004).

Lipases (EC 3.1.1.3) are in a family of enzymes that, in their natural environment, can catalyze the hydrolysis of triacylglyceral to glycerol and fatty acid. However, under appropriate conditions, lipases have shown to be very active catalysts in transesterification, alcoholysis, and esterification (Foresti & Ferreira, 2007). An important application of lipase is in industrial processes and products due to their high specificity, good rate of reaction, non-toxicity, and water solubility, which are major advantages over inorganic catalysts. However, the use of enzymes and other proteins has been limited due to their considerably unstable nature and the resulting requirement of stringent conditions, such as a particular pH and temperature. Immobilization onto matrix has become a widely used technique to overcome these problems. The immobilization may also enhance the operation lifetime, thermal stability, structural rigidity, and recoverability of the biocatalyst. Generally, the efficiency of enzyme immobilization is decided by the support

* Corresponding author at: Department of Chemistry, Faculty of Science, Mahidol University, 999 Phuttamonthon 4 Road, Salaya, Nakhon Pathom 73170, Thailand. Tel.: +66 2 441 9816x1138; fax: +66 2 441 0511.
E-mail addresses: scpsu@mahidol.ac.th, panya.sun@mahidol.ac.th (P. Sunintaboon).

0144-8617/$ – see front matter © 2012 Elsevier Ltd. All rights reserved.
http://dx.doi.org/10.1016/j.carbpol.2012.04.019

size or surface area. If lipase is immobilized on nanoparticle or submicron particle supports, which have high specific surface area and low diffusion resistance, this would improve the effectiveness of the catalyst considerably (Wu, Wang, Lou, & Dai, 2009).

Recently, spinning disk processing (SDP) emerges as a technology in process intensification, which provides uniform reaction conditions on a rotating disk, in contrast to traditional batch technology where conditions can vary across the dimensions of reaction vessel. SDP also provides rapid mixing and high contact between mixing components. The centrifugal force produces intense interfering waves, which generates high heat transfer between liquid solution and disk, and high mass transfer between the solution and air above the disk. The waves of starting materials generated on the disk form almost pure plug flow, causing every molecule to experience the same environment. In addition, the residence time is typically in seconds. Due to these reasons, SDP can lead to enormous improvement in reaction selectivity and outputs. Another novel feature of SDP is that it is a continuous flow process. Therefore, it can facilitate large scale production (Anantachoke et al., 2006).

In this work, the successful preparation of chitosan-functionalized PMMA particles by SDP was illustrated. The positively charged chitosan was coated on negatively charged PMMA particles as a result of electrostatic interaction and efficient mixing conditions provided by SDP. Then, the complexes obtained were subjected to various physico-chemical characterizations. The positive charges of outer chitosan layer were then used for lipase immobilization. Adsorption behavior of lipase on PMMA-CH particles was investigated by zeta potential measurements. The specific activity of free and immobilized enzymes was also investigated.

2. Materials and methods

2.1. Materials

Chitosan (from Seafresh Chitosan Lab., Thailand) solutions (1 wt%) of three molecular weights: 45, 100, and 230 kDa (abbreviated as CH45, CH100, and CH230, respectively) were prepared by dissolving the materials in 1 wt% acetic acid aqueous solution. Methyl methacrylate (MMA) monomer was purchased from Sigma–Aldrich and purified by distillation under reduced pressure and was stored at 4 °C before use. Potassium persulfate (KPS) was purchased from Fluka. It is an analytical grade reagent and used without further purification. Lipase AY (from *Candida rugosa*, lyophilized powder) was supplied by Amano Enzyme Co., Nagoya, Japan with the activity and the molecular weight of 32,800 U/g and 60,000 g/mol, respectively (Lot No. LAY E0151016). 1,2,3-Tributyrylglyceral (tributyrin) was purchased from Sigma–Aldrich. Gum arabic (Ga) was purchased from Ajax Finechem, New Zealand. Tris (hydroxymethyl) aminomethane (Tris) was purchased from Fisher Scientific U.K. Limited, United Kingdom. Distilled water was used for all experiments.

2.2. Preparation of negatively charged PMMA particles

Negatively charged PMMA particles were synthesized *via* a soap-free emulsion polymerization. Briefly, 40 g of distilled water and 3 g of MMA monomer were charged into a 100 mL three-necked round-bottom flask with a reflux condenser, and nitrogen inlet. After degassed for 30 min and the temperature of the reactor raised to 80 °C, then 7 g of aqueous KPS solution (9.16 mM) was added into the reactor. After feeding initiator, the polymerization was carried out at the same temperature for 3 h. Then, percentages of monomer conversion and solid content were determined gravimetrically. About 3 g of prepared latex was taken into a pre-weighed aluminum pan. After complete evaporation in a fume-hood, the air-dried latex was further dried in a vacuum oven at 70 °C. The percent monomer conversion and solid content were calculated (Inphonlek, Pimpha, & Sunintaboon, 2010).

2.3. Preparation of PMMA-CH core–shell particles

PMMA particle (1 wt%) dispersion was allowed to interact with 0.1, 0.5, and 1 wt% of chitosan solution on a spinning disk rector (SDR type-102 series, 100 mm diameter of the disk) *via* electrostatic interaction to obtain PMMA-CH core–shell particles. Both components were pumped to mix on the disk with feed rates of 1.0, 1.5, and 2.0 mL/s using 2.1 mm feed injection diameter. The speed levels of spinning disk were varied as 500, 1000, and 1500 rpm. After the optimum feed rate and spinning speed were obtained, the effect of chitosan molecular weights was studied. The complexed particles prepared from chitosan 45, 100, and 230 kDa were abbreviated as PMMA-CH45, PMMA-CH100, and PMMA-CH230 particles, respectively. In each mixing process on SDR, the mixture was collected from the product discharge panel.

2.4. Measurement of the mean particle size and zeta potential

The mean particle size and size distribution of neat PMMA and PMMA-CH particles were measured by dynamic light scattering (DLS) (MALVERN instruments) with the refractive index of 1.476 for neat PMMA and 1.590 for PMMA-CH particles. All DLS measurements were carried out at room temperature and in aqueous medium. A mechanical stirring was applied to enhance dispersibility of the sample. A background measurement was performed using distilled water before sample measurement to avoid background electrical noise. Then, the sample were dropped into the sample chamber until the suitable concentration was attained, which was in a range of 5–10 wt%. All results were the average of triplicate measurement.

Surface charges of PMMA-CH particles were determined on electrophoretic light scattering using zetasizer (zetasizer 3000, Malvern Instruments, UK). Samples were diluted with 1 mM NaCl solution at room temperature and measured in the automatic mode. All measurements were performed in triplicates.

2.5. Morphological characterization

The size and morphology of particles were also observed with transmission electron microscope (TEM, Phillip TECNAI 20). The particle dispersion was diluted fifty times with distilled water. An aliquot of 50 μL was then deposited on a copper grid and stained with 1.5 wt% phosphotungstic acid (PTA). The particle diameter was denoted with arithmetic average diameter. In addition, the information of particle size and morphology was investigated by scanning electron microscope (SEM, S-2500, Hitachi) and atomic force microscopy (AFM). To prepare the samples for SEM, particle dispersion was dropped on a cover glass and dried in a dust-free environment. The dried specimens were attached on the sample holders with a double-coated carbon conductive tape and then were sputter-coated under vacuum with platinum and palladium by using a sputter coater (E102, Hitachi, Japan). The sputter-coated samples were then observed by the microscope at 15 kV. For AFM, the particle dispersion with a suitable dilution in distilled water was dropped on a cover glass, and dried overnight. AFM images were observed in air with a Nanoscope IIIa (model Ns3a) operating in a tapping mode.

2.6. FT-IR spectroscopic analysis

Fourier-transform infrared (FTIR) spectroscopy (Perkin-Elmer, PE2000) was utilized to characterize the functional groups of

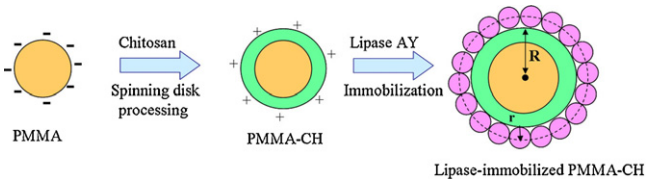

Scheme 1. Formation of PMMA-CH particles by spinning disk processing and their lipase immobilization.

samples and confirm the coating of chitosan onto colloidal PMMA particles. The scanning of each spectrum was done in the range between 4000 and 370 cm^{-1} with 4 cm^{-1} resolution.

2.7. Thermal property

Thermogravimetric analysis (TGA/SDTA851, Mettler, Switzerland) was conducted to study thermal stability of particles. The sample was accurately weighed about 8–12 mg in an aluminum pan. The measurement was conducted from 40 to 600 °C at a heating rate of 10 °C/min under a nitrogen and oxygen purge (flow rate 60 mL/min).

2.8. Immobilization of lipase AY on PMMA-CH core–shell particles

The protein content of lipase AY was 2.95 ± 0.33% as determined by the Lowry method (Bollag, Edelstein, & Rozycki, 1996). For immobilizing lipase AY on the positively charged surface of PMMA-CH particles, the procedure (as shown in Scheme 1) was followed: 1 mg/mL lipase solution (1, 3, and 5 mL) in 0.28 mM Tris–HCl pH 7.5 buffer was added progressively to a solution of 50 μL of PMMA-CH particles (final concentration of 1 wt%). The mixture was stirred at 300 rpm continuously for 30 min at room temperature. The immobilized particle dispersion was traced by using zetasizer.

To determine the percent lipase AY adsorption capacity (%*A*) on PMMA-CH particles, the hexagonal close-packing of lipase AY molecules on a planar surface was assumed. %*A* was calculated from Eq. (1):

$$\%A = \frac{N_l}{N_p S} \times 100 \quad (1)$$

where N_l, N_p, and S are the total number of lipase AY molecules, number of PMMA-CH particles per unit volume, and the number of lipase AY molecules covered as a monolayer on one PMMA-CH particle, assuming hexagonal close-packing. Since PMMA-CH particles were prepared *via* the complexation between PMMA particles and chitosan, the number of all PMMA-CH particles should be equal to that of starting PMMA particles. Therefore, the number of particles per unit volume of aqueous medium, N_p, can be calculated from Eq. (2) (Kin et al., 2010):

$$N_p = \frac{6m_p}{\pi D^3 d_p} \quad (2)$$

where m_p is the total mass of PMMA (per mL of aqueous phase) in the system, D is the average diameter of PMMA particles, which is 254 nm (from TEM), and d_p is the density of PMMA (1.178 g cm^{-3}). From the calculation, the N_p in 50 μL of PMMA or PMMA-CH particles was 4.95×10^{10} particles. Since lipase is considered to be spherical in shape, which has 4 nm in diameter, the number of lipase per one PMMA-CH particle can be calculated from Eq. (3) (Ottewill, Schofield, Waters, & Williams, 1997):

$$S = \frac{4\pi(R+r)^2}{2\sqrt{3}r^2} \quad (3)$$

where R and r are the radii of PMMA-CH particle and lipase AY, respectively.

2.9. Determination of lipase AY activity

A modified assay, using pH-stat method as described by Kaewprapan, Tuchinda, Marie, Durand, and Inprakhon (2007), was used to determine the activity of lipase AY and lipase AY-immobilized PMMA-CH core–shell particles. Tributyrin (20 mM) substrate was added into 20 mL of Tris–HCl buffer containing 2% of gum arabic and an emulsion of substrate was made with a homogenizer (IKA Ultra Turrax T25, IKA Labortechnik, USA) for 20 s at 10,000 rpm. The operation was repeated 3 times. Then the temperature and pH of the solution in pH-stat titrator (Mettler toledo DL50, Schwerzenbach, Switzerland) were adjusted to 37 °C and 7.5, respectively. After adding 1 mL of 1 mg/mL lipase AY solution, the enzyme activity was measured by titrating the released fatty acid with 0.01 N sodium hydroxide solution using a pH-stat titrator. The initial velocity was determined from the slope of linear plot of fatty acid concentration against time. The same experiment was repeated 2 times and the average initial velocity was determined. The control reaction was performed without enzyme. One enzyme unit hydrolyzes 1.0 micro equivalent of fatty acid from a triglyceride in 1 min at pH 7.5 and 37 °C.

3. Results and discussion

3.1. Optimization of SDP

In general, SDP involves a mixing of reactants as molecularly dispersed solutions on the surface of a rotating disk (see S.I. 1 in Supporting information). Some SDP parameters can affect such mixing process. Therefore, the optimum sample feed rate and disk speed rate should be first obtained before further operation. The reactants used in this part were chitosan 100 kDa, and 1 wt% PMMA particle dispersion (monomer conversion = 94% and zeta potential = −75 mV). On the variation of feed rate (1, 1.5, and 2 mL/s), it was found that the feed rate of 1 mL/s was too slow for chitosan 100 kDa solution used, since its viscosity might be too high. When the feed rates were increased as 1.5 and 2 mL/s, both chitosan 100 kDa solution and PMMA particle dispersion can flow smoothly. As observed from size distribution profiles, both higher feed rates resulted in the uniform distribution (S.I. 2 in Supporting information). The feed rate of 1.5 mL/s was selected for further fine tuning the disk speed rate, which was varied as follows: 500, 1000, and 1500 rpm. The results showed that all disk speed rates yielded PMMA-CH100 particles with quite narrow size distribution (S.I. 2 in Supporting information). However, the disk speed rate of 1000 rpm was chosen for further complexation step because it yielded the narrowest size distribution. In fact, an independent direct adsorption of chitosan on PMMA-CH particles by mixing them by a conventional method was carried our (in a beaker with a magnetic stirrer for 10 and 30 min of mixing time, at 600 rpm stirring rate). It was found that at the mixing condition above, the

Table 1
Effect of various weight ratios of PMMA to chitosan on mean particle size and zeta potential.

PMMA:Chitosan (wt%)	Mean particle size (nm)	Zeta potential (mV)
1.0:0.0	275 ± 1	−75.4 ± 1.0
1.0:0.1 (CH 45 kDa)	305 ± 5	49.9 ± 0.6
1.0:0.5 (CH 45 kDa)	301 ± 8	49.5 ± 1.0
1.0:1.0 (CH 45 kDa)	302 ± 9	48.5 ± 0.2
1.0:0.1 (CH 100 kDa)	313 ± 5	45.9 ± 0.6
1.0:0.5 (CH 100 kDa)	320 ± 4	51.5 ± 0.7
1.0:1.0 (CH 100 kDa)	315 ± 6	63.2 ± 0.5
1.0:0.1 (CH 230 kDa)	325 ± 12	51.7 ± 0.3
1.0:0.5 (CH 230 kDa)	305 ± 5	54.4 ± 1.1
1.0:1.0 (CH 230 kDa)	324 ± 5	55.1 ± 1.4

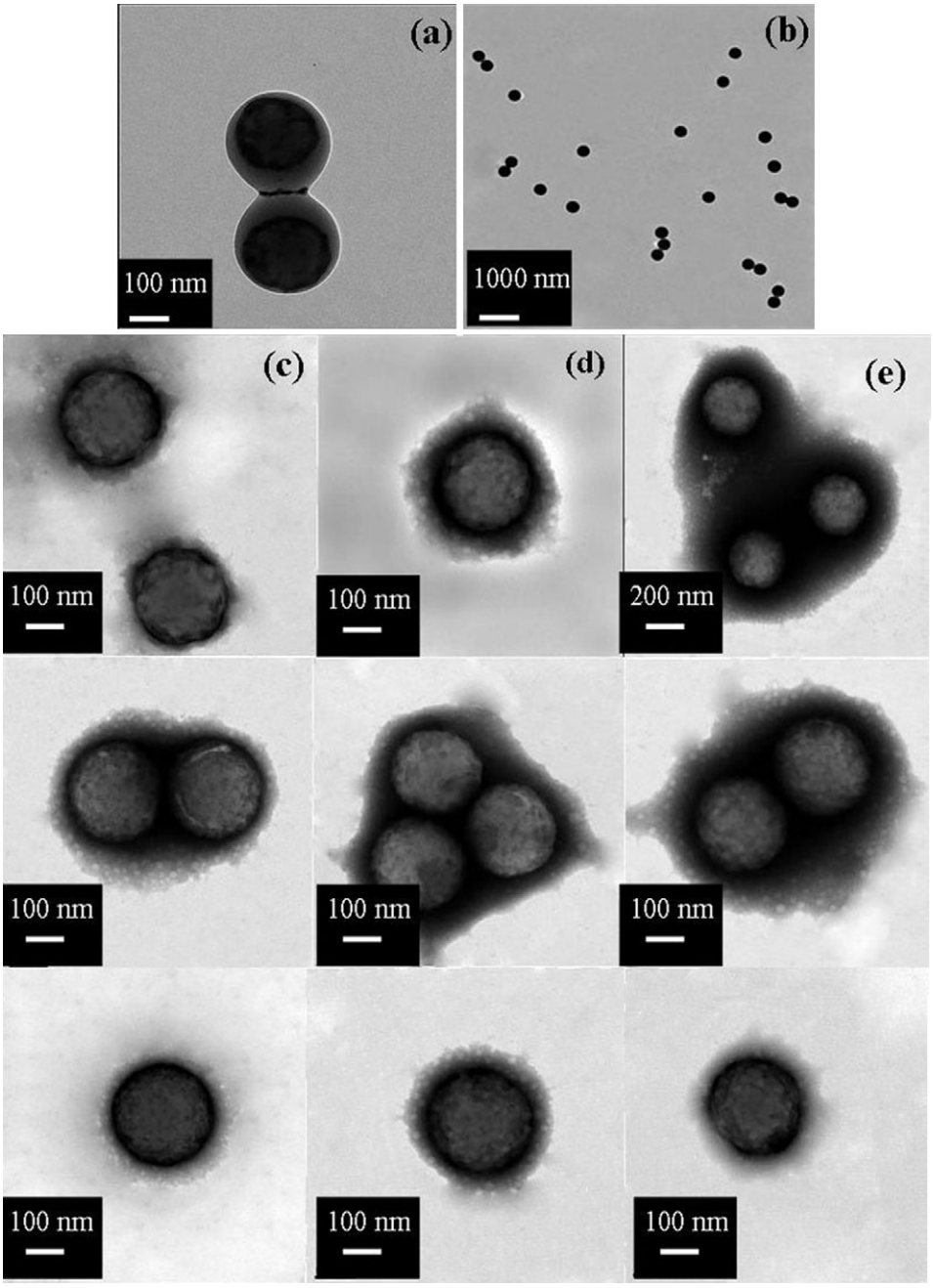

Fig. 1. TEM micrographs of PMMA (a) 25,000× and (b) 2500× and of PMMA-CH core–shell particles at various ratios of PMMA:CH; 1:0.1, 1:0.5, and 1:1 wt% (top to bottom) (c) CH 45 kDa, (d) CH 100 kDa, and (e) CH 230 kDa.

resulting particles had the sizes 714 nm, and 539 nm for the mixing times 10 and 30 min, respectively, which were larger than that of lean PMMA particles and decreased with the mixing time. In addition, the positive zeta potentials (∼+60 mV) were obtained. Although larger size and positive zeta potentials, which are the indication of adsorption of chitosan on PMMA particles, can be observed at the condition above, the mixing time seemed to have a dramatic effect and is needed to be fine-tuned. Compared to a spinning disk processing, this conventional mixing is required much longer time. Moreover, the stirring rate including concentration and quantity of each component is expected to have an influence on the adsorption. Even though the ordinary mixing could also cause the adsorption between anionic particles and cationic polymer, it is certain that SDP could provide superior characteristics over the ordinary one by many reasons mentioned in the introduction part.

3.2. Preparation and characterization of PMMA-CH core–shell particles

PMMA particles (1 wt%) were subjected to react electrostatically with chitosan solutions of three molecular weights and three concentrations (0.1, 0.5, and 1 wt%) for each chitosan molecular weight on the SDR at the conditions of 1.5 mL/s sample feed rate and 1000 rpm disk speed rate. As illustrated in Table 1, compared to the lean PMMA particles (275 nm), the complexation between PMMA particles (1 wt%) and chitosan solutions (0.1, 0.5, and 1 wt%) resulted in the larger size particles, which were in the range of 301–325 nm. From zeta potential measurement, it was found that after complexation, the charges were altered from −75.4 to +45.9 mV or higher (up to +63.2 mV), depending on the molecular weight of chitosan. From the changes of size and surface

charge, it was evident that the positively charged chitosan could be coated on the negatively charged PMMA colloidal particles *via* electrostatic interaction. Moreover, it can be observed that the concentration of chitosan had not much effect on mean particle sizes and zeta potentials. Nevertheless, the average sizes and zeta potentials tended to increase with molecular weight of chitosan. Also, pH values of medium were found to influence the hydrodynamic diameters of the complexed particles. The change of pH values of the medium from 3 to 10 led to a gradual decrease of their hydrodynamic sizes from 334 to 220 nm in diameter (S.I. 3 in Supporting information). In an acidic environment, amine groups on chitosan can be protonated causing an expansion of chitosan chains (Leung, Zhu, Harris, & Li, 2004). Therefore, the decrease in size of PMMA-CH particles at higher pHs might be from the shrinkage of chitosan chains as a result of deprotonation. However, from zeta potential values in Table 1, all of complexed particles showed positive surface charges indicating the presence of chitosan on their surfaces, which would be capable of immobilizing negatively charged species.

The morphology of PMMA and PMMA-CH particles was observed using TEM. PMMA particles had the average diameter approximately 254 nm, and possessed spherical shape and smooth surface as shown in Fig. 1(a). In contrast, PMMA-CH particles had the additional hairy layer on their surfaces that was a strong evidence showing that chitosan wrapped around the PMMA colloidal particles. It was also found that when the molecular weights of chitosan increased the particle size of the PMMA-CH particles also increased (as determined from Fig. 1(c)–(e)). The additional information from AFM and SEM also supported their size and shape (S.I. 4 and 5 in Supporting information).

FT-IR spectra of pure chitosan, PMMA, and PMMA-CH100 core–shell particles were acquired to observe and compare the changes in their chemical functional groups before and after complexation (Fig. 2). The spectrum of chitosan exhibited the characteristic peaks of amide II (N—H deformation in plane) at 1600 cm^{-1} due to the remaining acetamide groups in the chitosan. The broad peak appeared in a range of 3100–3600 cm^{-1} corresponding to O—H and N—H stretching. The strong peak around 1150–1200 cm^{-1}, which corresponded to C—O stretching in ether linkages, was also observed. The signals at 2880 and 1384 cm^{-1} were assigned to C—H stretching and CH_3 symmetric deformation, respectively (Chen, Wang, & Lin, 2002). The absorption peak appearing at 1736 cm^{-1} was assigned for the carbonyl absorption from methacrylate groups on PMMA particles (Wang, Yan, Cui, Cong, & Wang, 2010). In the spectrum of PMMA-CH100 core–shell particles, the presence of additional N—H deformation at 1600 cm^{-1} to the carbonyl absorption at 1736 cm^{-1} could confirm the complexation between PMMA and chitosan.

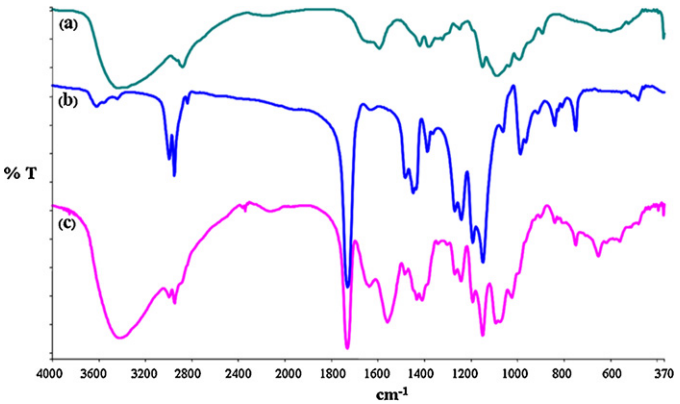

Fig. 2. FT-IR spectra of (a) CH, (b) PMMA, and (c) PMMA-CH core–shell particles.

Table 2
Zeta potential values of lipase-immobilized PMMA-CH core–shell particles.

PMMA-CH particles (μL)	Crude lipase (mL)	Buffer (mL)	Zeta potential (mV)		
			PMMA-CH45	PMMA-CH100	PMMA-CH45
50	0	20	53.2	57.6	54.1
50	1	19	34.1	31.7	31.7
50	3	17	30.8	25.0	26.3
50	5	15	19.8	20.2	18.2

Their thermal stability was investigated by TGA. The thermograms of chitosan powder, PMMA, and PMMA-CH particles were obtained under O_2 and N_2 atmosphere (as shown in S.I. 6 in Supporting information). The TGA thermogram of chitosan showed a two-step weight loss. The first step ranged between 40 and 180 °C and showed about 12% loss in weight. This would correspond to the loss of bound water. The second step started at 200 °C and continued up to 450 °C with 52% weight loss due to the degradation of chitosan (Huacai, Wan, & Dengke, 2006). The decomposition of PMMA also exhibited a two-step degradation behavior that occurred in the temperature ranges 100–330 and 330–440 °C, respectively (Peterson, Vyazovkin, & Wight, 1999). The first step can be associated with chain scission at the relatively weak bonds such as a head-to-head linkage. The second step may correspond to an unzipping from the unsaturated end groups and random chain scissions with the polymer chains (Ninjbadgar, Yammamoto, & Takano, 2007). Residue percent was approximately 36%. The TGA curves of PMMA-CH particles prepared from 3 different molecular weights of chitosan were similar and had a combination of degradation behavior of both pure chitosan and lean PMMA. This was also supported the presence of both components in the complexed particles.

3.3. Lipase immobilization on PMMA-CH core–shell particles

In order to investigate the ability of PMMA-CH particles to immobilize negatively charged species, the lipase AY was selected as a negatively charged model. Because the lipase AY possesses negative charges when it is in the environment that is over its isoelectric point (p*I* = 4.3), it can interact easily with positively charged PMMA-CH particles *via* electrostatic attraction. Zeta potential measurement was performed to trace their interaction. Since the crude lipase powder used has a protein content of 2.95 wt% with a molecular weight of 60,000 g/mol, therefore, it has 3×10^{19} lipase molecules per 1 mg of the crude powder. At a fixed amount of PMMA-CH particles (50 μL), when the amount of 1 mg/mL crude lipase was varied from 0 to 5 mL, the zeta potential values of resulting lipase-immobilized PMMA-CH particles decreased for all of PMMA-CH particles used as shown in Table 2. This is the evidence

Table 3
Percentage of lipase AY adsorption capacity (%*A*) on PMMA-CH particles at various protein contents.

Crude lipase (1 mg/mL) (mL)	Lipase content (mg)	Number of lipase (molecule)	Lipase AY adsorption capacity (%)		
			PMMA-CH45[a]	PMMA-CH100[b]	PMMA-CH230[c]
1	0.03	3×10^{14}	34	32	30
3	0.08	8×10^{14}	93	86	81
5	0.15	15×10^{14}	175	161	152

[a] Number of lipase AY molecules on one PMMA-CH45 particle is 17,426 molecules.
[b] Number of lipase AY molecules on one PMMA-CH100 particle is 18,936 molecules.
[c] Number of lipase AY molecules on one PMMA-CH230 particle is 20,018 molecules.

that negatively charged lipase could be immobilized on the PMMA-CH particles, leading to the lower surface charges. Table 3 shows the percent lipase adsorption capacity on PMMA-CH particles at various protein contents. With an assumed close-packed monolayer of lipase AY on the surface of PMMA-CH particles, the lipase molecules covering one PMMA-CH particle (S) can be determined from Eq. (3). The radius (R) of PMMA-CH particles used for this calculation was obtained by DLS measurement (Table 1). The percentage of lipase AY adsorption capacity (%A) can then be obtained from Eq. (1). It was found that when the amount of crude lipase increased from 1 to 3 mg, the %A increased from 30–34% to 81–93% for all the prepared PMMA-CH particles. When the amount of crude lipase was 5 mg, the adsorption capacity was exceeded 100% (152–175%). From the additional calculation, the amounts of lipase AY required to cover on one PMMA-CH particle were 0.086, 0.094, and 0.097 mg for PMMA-CH45, PMMA-CH100, and PMMA-CH230 particles, respectively. Thus, about 0.10 mg of lipase AY should saturate the surface of all PMMA-CH particles at 50 μL. With 0.03 mg of lipase AY supplied (from 1 mL of 1 mg/mL crude lipase), a total adsorption of those lipases on PMMA-CH particles with %A around 30% was occurred since the amount of lipase given were quite low comparing to the available particles' surface. When increasing the amount of lipase to 0.08 mg, %A can reach the values higher than 80% (up to 93% for PMMA-CH45 particles). However, the further increase of lipase to 0.15 mg led to over 100% lipase AY adsorption capacity, which obviously indicated that the assumption of hexagonal close-packing of lipase AY molecules monolayerly covered on a planar surface might not be valid for this lipase concentration. The surplus lipases might aggregate onto themselves *via* unspecific binding or might partition into the continuous phase. It also emerges from this study that the lipase AY adsorption capacity values tended to decrease with higher molecular weight of chitosan used, as shown in Table 3. The reason is because the particle sizes of the PMMA-CH particles were different. The particle size of PMMA-CH45 particles was smaller than that of PMMA-CH100 and PMMA-CH230 particles, leading to the lower S values, which in turn, the higher %A (from Eq. (1))

Naturally, lipases can catalyze the hydrolysis of fats and oils (triglyceride) to be fatty acid and glycerol *via* a Ser-His-Asp/Glu catalytic triad active site. The adsorption of free enzyme on the microparticles leads inevitably to "dilution of activity" due to the introduction of a large portion of non-catalytic ballast, ranging from 90% to >99% (Tischer & Kascher, 1999). The immobilization of an enzyme on a carrier often leads to the loss of more than 50% of native activity, especially at high enzyme loading (Bryjak & Kolarz, 1998). The effect of immobilization on the activity can be evaluated by studying the lipase activity prior to and after immobilization. As lipases catalyzed the hydrolysis of triglyceride in nature, olive oil and tributyrin are used as the reference substrates for the determination of lipase activity (Jaeger, Dijkstra, & Reetz, 1999). In this study, tributyrin was first prepared in the form of emulsified substrate for assaying the activities of free lipases and immobilized lipases. The progress curve of free lipase AY, and lipase AY-immobilized on PMMA-CH100 particles catalyzed hydrolysis of emulsified tributyrin under the same reaction conditions were illustrated in Fig. 3. The general mechanism of hydrolysis composes of four steps and was reported elsewhere (Jaeger et al., 1999).

The initial velocity of hydrolysis reaction catalyzed by free lipase AY at 0.03, 0.08 and 0.15 mg of lipases were determined to be 1.07, 2.46 and 3.81 μmol/min (listed in Table 4). Compared to free lipase, the activity of lipase AY immobilized onto the particles was approximately 2 times less than that of free lipase AY for every lipase concentration used, as shown in Fig. 4 and Table 4. This is very advantageous compared to the immobilization of lipases onto microparticles of which the enzyme activity was generally decreased up to 50%, as described above. It was clear that the

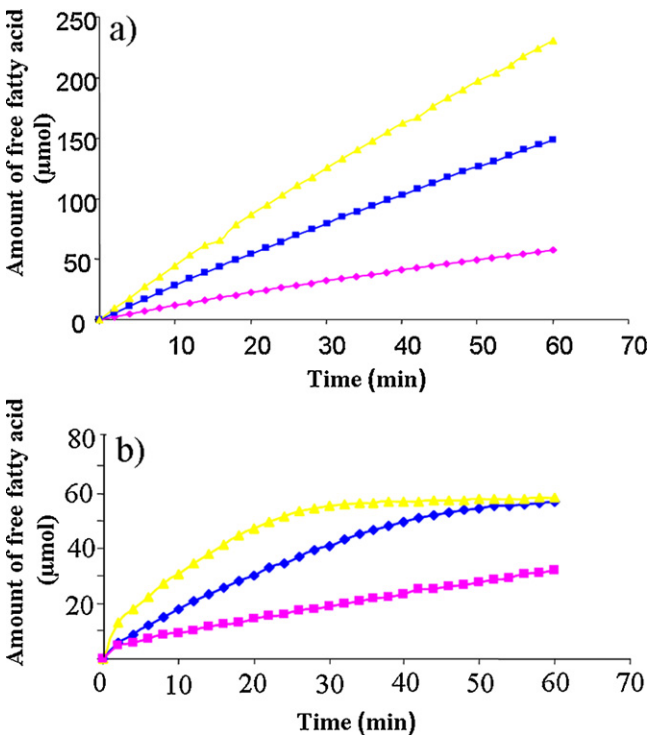

Fig. 3. Progress curves of the reaction over time of (a) free lipase and (b) lipase AY-immobilized PMMA-CH100 catalyzed hydrolyzes of emulsified tributyrin; (■) 1 mL lipase AY/PMMA-CH particles + 1 mL lipase AY, (◆) 3 mL lipase AY/PMMA-CH particles + 3 mL lipase AY, and (▲) 5 mL lipase AY/PMMA-CH particles + 5 mL lipase AY.

Table 4
Activity and specific activity of free lipase of lipase-immobilized PMMA-CH100 particles.

Sample	Activity (μmol/min)			Specific activity (μmol/min mg protein)		
	1 mL lipase	3 mL lipase	5 mL lipase	1 mL lipase	3 mL lipase	5 mL lipase
Free lipase	1.07	2.46	3.81	36.36	27.77	25.81
lipase-immobilized PMMA-CH100	0.46	1.24	1.88	15.62	14.06	12.74

immobilization of lipase AY on the submicron-sized particles may lead to a steric restriction for lipase to move to the surface of tributyrin oil, or conformation alteration of lipase. In regard to the lipase AY immobilized on PMMA-CH100 particles, an increase in catalyst loading from 0.03 to 0.15 mg led to the linear increase in initial velocity as shown in Fig. 4 and listed in Table 4. The increase in

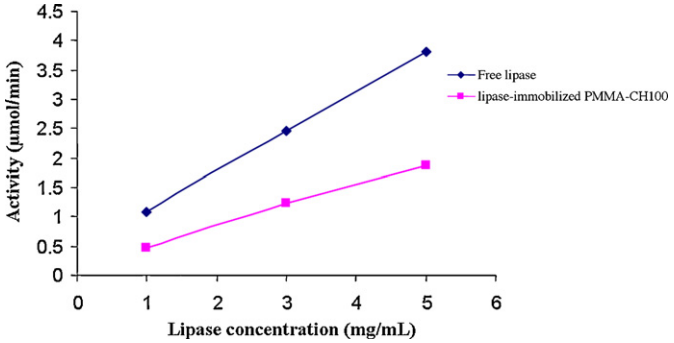

Fig. 4. Activity of (◆) free lipase AY and (■) lipase-immobilized PMMA-CH100 particles.

initial velocity as a function of lipase loading was less pronounced when the lipase load was increased from 0.08 mg to 0.15 mg. This might be to the saturation of particles at 0.15 mg of lipases, as described previously. On the other hand, a specific activity of both free lipase AY and lipase AY immobilized on the particles decreased with increasing amount of lipase loading as shown in Table 4. The reason for the loss of specific activity may be due to ratio of lipase to substrate was too high and the saturation was already reached.

The immobilization of enzymes on a solid support is expected to result in the enzymes' structure stabilization, make them more robust, and more resistance to environmental change. Thus, the enzymes' stability immobilized is one of prime matter to be concerned. In general, the stability level of enzymes, including lipase, depends on their capacity of maintaining their 3-dimensional structure in the solution. In addition, pH and ionic strength of medium are also the very important factors that could affect the rate and conversion of lipases-catalyzed hydrolysis of fats. For fat cleavage, the ionic strength needs to be at a medium to high value to favor the rapid adsorption of lipases on the hydrophobic fat–water interface and to clean the insoluble fatty acid products from the interface. In this present work, the immobilization of lipase AY on PMMA-CH was carried out at the ionic strength of 154 mM, which is still in the suitable the range for enzymatic fat cleavage process as investigated by our group [S.I. 7 in Supporting information]. In regard to the pH of the medium, it needs to be higher than pK_a of fatty acid (pH about 7.6–9.85) to make the fatty acid ionized and more soluble in water. In addition, the stable pH range of lipase AY is known to be 5.0–8.0. Based on the information given above, it's quite certain that lipase AY immobilized on PMMA-CH particles should be sufficiently stable However, the operational conditions (*e.g.* pH, buffer ionic strength) that could affect the stability and activity of lipase immobilized on PMMA-CH particles will be carried out systematically in more specific ways in the forthcoming stage.

4. Conclusion

The chitosan-functionalized PMMA particles were conveniently prepared by using the SDP, where the effective complexation of anionic PMMA colloidal particles and cationic chitosan occurred. Bioconjugation of PMMA-CH core–shell particles with lipase AY leads to a new class of biocatalyst that combines the utility of immobilization in terms of reuse with easy access of substrate to the enzyme. Residued activity of lipase AY immobilized on the particles makes it ideally suitable for the economic production of immobilized biocatalysts for the industrial applications such as the manufacture of fatty acid by the hydrolysis of triglyceride.

Acknowledgments

This work was financially supported by Mahidol University and the Center of Excellence for Innovation in Chemistry (PERCH-CIC), the Office of Higher Education Commission, Ministry of Education, Thailand.

Appendix A. Supplementary data

Supplementary data associated with this article can be found, in the online version, at http://dx.doi.org/10.1016/j.carbpol.2012.04.019.

References

Anantachoke, N., Makha, M., Raston, C. L., Reutrakul, V., Smith, N. C., & Saunders, M. (2006). Fine tuning the production of nanosized α-carotene particles using spinning disk processing. *Journal of the American Chemical Society*, *128*, 13847–13853.
Bollag, D. M., Edelstein, S. J., & Rozycki, M. D. (1996). *Protein methods* (2nd ed.). New York: Wiley-Liss Inc.
Bryjak, J., & Kolarz, B. N. (1998). Immobilization of trypsin on acrylic copolymer. *Process Biochemistry*, *33*, 409–417.
Caruso, F., Lichtenfeld, H., Giersig, M., & Mohwald, H. (1998). Electrostatic self-assembly of silica nanoparticle-polyelectrolyte multilayers on polystyrene latex particles. *Journal of the American Chemical Society*, *120*, 8523–8524.
Chen, F., Wang, Z., & Lin, C. (2002). Preparation and characterization of non-sized hydroxyapatite particles and hydroxyapatite/chitosan nano-composite for use in biomedical materials. *Materials Letters*, *57*, 858–861.
Chiou, S. H., & Wu, W. T. (2004). Immobilization of *Candida rugosa* lipase on chitosan with activation of the hydroxyl groups. *Biomaterials*, *25*, 197–204.
Foresti, M. L., & Ferreira, M. L. (2007). Chitosan-immobilized lipases for the catalysis of fatty acid esterifications. *Enzyme and Microbial Technology*, *40*, 769–777.
Huacai, G., Wan, P., & Dengke, L. (2006). Graft copolymerization of chitosan with acrylic acid under microwave irradiation and its water absorbency. *Carbohydrate Polymers*, *66*, 372–378.
Inphonlek, S., Pimpha, N., & Sunintaboon, P. (2010). Synthesis of poly(methyl methacrylate) core/chitosan-mixed-polyethyleneimine shell nanoparticles and their antibacterial property. *Colloids and Surfaces B: Biointerfaces*, *77*, 219–226.
Jaeger, K. E., Dijkstra, B. W., & Reetz, M. T. (1999). Bacterial biocatalysts: Molecular biology, three-dimensional structures and biotechnological applications of lipases. *Annual Review Microbiology*, *53*, 315–351.
Jia, Y., Hu, Y., Zhu, Y., Che, L., Shen, Q., Zhang, J., et al. (2011). Oligoamines conjugated chitosan derivatives: Synthesis, characterization, *in vitro* and *in vivo* biocompatibility evaluation. *Carbohydrate Polymers*, *83*, 1153–1161.
Kaewprapan, K., Tuchinda, P., Marie, E., Durand, A., & Inprakhon, P. (2007). pH-imprinted lipase catalyzed synthesis of dextran fatty acid ester. *Journal of Molecular Catalysis B: Enzymatic*, *47*, 135–142.
Kin, M. H., Wei, Y. L., Cheng, H. L., Chun, H. Y., Gilbert, R. G., & Li, P. (2010). Mechanistic study of the formation of amphiphilic core–shell particles by grafting methyl methacrylate from polyethylenimine through emulsion polymerization. *Polymer*, *51*, 3512–3519.
Krajewska, B. (2004). Application of chitin- and chitosan-based materials for enzyme immobilizations: A review. *Enzyme and Microbial Technology*, *35*, 126–139.
Leung, M. F., Zhu, J., Harris, F. W., & Li, P. (2004). New route to smart core–shell polymeric microgels: Synthesis and properties. *Macromolecular Rapid Communications*, *25*, 1819–1823.
Li, P., Zhu, J., Sunintaboon, P., & Harris, F. W. (2002). New route to amphiphilic core–shell polymer nanospheres: Graft copolymerization of methyl methacrylate from water-soluble polymer chains containing amino groups. *Langmuir*, *18*, 8641–8646.
Marie, E., Landfester, K., & Antonietti, M. (2002). Synthesis of chitosan-stabilized polymer dispersions, capsules and chitosan grafting products via miniemulsion. *Biomacromolecules*, *3*, 475–481.
Muzzarelli, C., Francescangeli, O., Tosi, G., & Muzzarelli, R. A. A. (2004). Susceptibility of dibutyryl chitin and regenerated chitin fibres to deacrylation and depolymerization by lipase. *Carbohydrate Polymers*, *56*, 137–145.
Muzzarelli, R. A. A. (2009). Genipin-crosslinked chitosan hydrogels as biomedical and pharmaceutical aids. *Carbohydrate Polymers*, *77*, 1–9.
Ninjbadgar, T., Yammamoto, S., & Takano, M. (2007). Thermal properties of the γ-Fe_2O_3/poly(methyl methacrylate) core/shell nanoparticles. *Solid State Sciences*, *7*, 33–36.
Ottewill, R. H., Schofield, A. B., Waters, J. A., & Williams, N. St. J. (1997). Preparation of core–shell polymer colloid particles by encapsulation. *Colloid and Polymer Science*, *275*, 274–283.
Peterson, J. D., Vyazovkin, S., & Wight, C. A. (1999). Kinetic study of stabilizing effect of oxygen on thermal degradation of poly(methyl methacrylate). *Journal of Physical Chemistry B*, *103*, 8087–8092.
Tischer, W., & Kascher, V. (1999). Immobilized enzymes: Crystals or carriers? *Trends in Biotechnology*, *17*, 326–335.
Torrado, S., Prada, P., De la Torre, P. M., & Torrado, S. (2004). Chitosan-poly(acrylic) acid polyionic complex: In vivo study to demonstrate prolonged gastric retention. *Biomaterials*, *25*, 917–923.
Wang, C., Yan, J., Cui, X., Cong, D., & Wang, H. (2010). Preparation and characterization of magnetic hollow PMMA nanospheres via in situ emulsion polymerization. *Colloids and Surfaces A: Physicochemical and Engineering Aspects*, *363*, 71–77.
Wu, Y., Wang, Y. J., Lou, G. S., & Dai, Y. Y. (2009). In situ preparation of magnetic Fe_3O_4-chitosan nanoparticles for lipase immobilization by cross-linking and oxidation in aqueous solution. *Bioresource Technology*, *100*, 3459–3464.